Chinese Physics C

Effects due to a Pu-C source on a HPGe detector and the corresponding neutron shielding[*]

ZHANG Jian-Yong(张建勇)[1;1)]   FU Cheng-Dong(傅成栋)[1]   MO Xiao-Hu(莫晓虎)[1;2)]

ZHANG Zi-Liang(张子良)[1,2]   LI Dao-Wu(李道武)[1]   WANG Bao-Yi(王宝义)[1]

[1] Institute of High Energy Physics, CAS, Beijing 100049, China
[2] Chengdu Science and Technology University, Chengdu 610059, China

Abstract: A gamma spectrum of a Pu-C source is measured using a p-type HPGe detector, whose three peaks (full energy, single-escape and double-escape peak) can be used as a calibration source for the beam energy measurement system of BEPCII. The effect of fast neutron damage on the energy resolution of the HPGe detector is studied, which indicates that the energy resolution begins to deteriorate when the detector is subject to 2×10^7 n/cm^2 fast neutrons. The neutron damage mechanism and detector repair methods are reviewed. The Monte Carlo simulation technique is utilized to study the shielding of the HPGe detector from the fast neutron radiation damage, which is of great significance for the future commissioning of the beam energy measurement system.

Key words: Pu-C source, HPGe detector, neutron shielding

PACS: 07.85.Fv, 61.80.Hg, 28.41.Te   **DOI:** 10.1088/1674-1137/35/7/011

1   Introduction

A large data sample to be collected at BESIII is typically a few fb^{-1} [1, 2], unprecedented statistical precision will be achieved in data analysis, hence many systematic factors and effects have to be seriously considered in order to obtain precise results. The detailed Monte Carlo simulation indicates [3–5] that the uncertainty of the beam energy plays an important role for BESIII physics analysis in many aspects. First of all, uncertainty due to the beam energy will be a bottleneck issue for further improvement of τ mass measurement. Secondly, such uncertainty is a crucial part of further high accuracy measurement of resonance parameters at BESIII. Lastly, the small systematic uncertainty of the beam energy is also an indispensable factor for the improvement of the branching ratio measurement aiming at an accuracy of 1%–2%.

Therefore, the high accuracy beam energy mea-

surement system has been designed [6] and is being constructed at the north crossing point (NCP) of the BEPC II [7]. The working principle of this system can be recapitulated as follows [8]: firstly, the source provides the laser beam and the optics system focuses the laser beam and guides it to make head-on collisions with the electron (or positron) beam in the vacuum pipe, after that the backscattering high energy photon or γ-ray will be detected by a High Purity Germanium (HPGe) detector.

The great merit of such a process consists in two aspects: firstly, there is a sharp Compton edge, which can be measured with fairly high accuracy by the HPGe detector. Secondly, as indicated by the formula [9, 10]

$$E_e = \frac{E_\gamma}{2}\left[1 + \sqrt{1 + \frac{m_e^2}{\epsilon_\gamma E_\gamma}}\right]\ ,\qquad(1)$$

there is an analytical relation between the energies of the laser beam (ϵ_γ), the electron beam (E_e), and the

backscattering γ-ray (E_γ). Since the energy of the laser beam (ϵ_γ) and the electron mass (m_e) are determined with the accuracy at the level of 10^{-8}, utilizing Eq. (1), E_e can be determined to be as accurate as E_γ, the accuracy of which is at the level of 10^{-5}. To this end, scrupulous calibration of the HPGe detector with the radiative sources is indispensable.

The designed beam energy of the BEPC II [7] ranges from 1 GeV to 2.3 GeV and the corresponding energy range for the backscattering photon is from 2 MeV to 7 MeV [11]. The calibration sources should cover this energy range. Many well-known radiative sources, such as ^{137}Cs, ^{60}Co and ^{24}Na can be used for calibration of the low and medium energy region (<3 MeV), as far as the high energy region (especially when the energy is greater than 5 MeV) is concerned, the Plutonium Carbon (Pu-C) [12, 13] source is almost the only choice.

In this paper, gamma spectroscopy of a Pu-C source is undertaken, the results of which will indicate if such a source is indeed suitable for energy calibration. The neutron damage due to the Pu-C source on a HPGe detector is studied in details. Since radiation shielding is necessary for the safety of HPGe, a Monte Carlo simulation is employed to test the effects of some protective materials. Last, the implication of the neutron damage on future energy measurement systems is discussed.

2 Introduction on experiments

The Pu-C source and the HPGe detector are the main components for the experiments described in this paper. In addition, a spectrometer system is also needed to measure the gamma spectrum.

2.1 Pu-C source

A Pu-C source is widely used as a calibration source for gamma and neutron detectors in the high energy region. Its 6130 keV gamma ray is produced by ^{13}C$(\alpha,$n$)^{16}$O reaction. The ^{238}Pu is used as an α emitter, two main α rays of 5.499 MeV and 5.455 MeV are emitted from the reaction:

$$^{238}\text{Pu} \rightarrow ^{234}\text{U} + \alpha \ (5.499 \text{ MeV, } 5.455 \text{ MeV}), \quad (2)$$

which are greater than the ^{16}O 6.13 MeV excited state and lower than the 6.92 MeV and 7.12 MeV excited states. An α particle is captured by ^{13}C:

$$\alpha + ^{13}\text{C} \rightarrow \text{n} + ^{16}\text{O}^* \quad (3)$$

followed by a neutron and an ^{16}O* state, where ^{16}O* indicates the 0^+ ground state, the 0^+ first ex-

cited state and the 3^- excited state. The gamma of 6130 keV is produced only when the 3^- excited state decays. The ratio of gamma to neutron is about 4.5% [14], and the neutron flux rate of the Pu-C source is 2.0×10^4 n/s in a 4π geometry. The structure of the Pu-C source used in this experiment is depicted in Ref. [15], also the energy spectrum of the neutron has been measured using a liquid scintillator. According to Ref. [15], there are three peaks at 3.8 MeV, 5.3 MeV and 7.1 MeV, respectively, in the neutron spectrum, most of the neutrons are fast neutrons.

Besides the Pu-C source, a ^{60}Co source is also adopted for energy calibration in this study.

2.2 HPGe detector

Germanium detectors are semiconductor diodes with a P-I-N structure in which the intrinsic region is sensitive to ionizing radiation, particularly X-rays and γ-rays. There are three types of reaction that happen in germanium semiconductor: the photoelectric effect, Compton scattering and pair production [16]. The latter two processes dominate when the energy of the injection photon is greater than 1 MeV. The germanium has a net impurity level of around 10^{10} atoms/cm^3 (an extremely small relative net impurity concentration compared to 4×10^{22} Ge atoms/cm^3 [16]) so that with a moderate reverse bias voltage, the intrinsic region that is the entire volume between the electrodes is depleted, and an electric field extends across this active region. When photons interact with the material within the depleted volume of a detector, charge carriers (holes and electrons) are produced and are swept by the electric field to the P and N electrodes. This charge, which is in proportion to the energy deposited in the detector by the incoming photon, is converted into a voltage pulse by an integral charge sensitive preamplifier. Subsequent amplification and pulse height analysis adds the pulse to an accumulated histogram, which eventually becomes the characteristic spectrum of the source.

At BEPC II the coaxial germanium detector (referred to as HPGe hereafter) will be adopted, which is basically a cylinder of germanium with an n-type contact on the outer surface, and a p-type contact on the surface of an axial well. The effective energy range of HPGe is from 50 keV to more than 10 MeV, which is satisfactory for beam energy measurement at BEPC II [8].

2.3 Geometry of setup

The source-detector geometry, used for obtaining

the gamma spectrum of the Pu-C source is shown in Fig. 1. The Ge crystal (ϕ 54.0 mm×50.2 mm, OR-TEC) is enclosed within a lead cylinder with inner-diameter 28 cm, height 60 cm and thickness 15 cm. The Pu-C source was placed directly at the top of detector along the cylindrical center axis of the Ge crystal. The distance between the source and the detector varies for different situations. For the source study, the distance is 1 cm and only a filter of 2 mm lead

plate is inserted between the source and the detector to suppress the detection of the low energy gamma rays. As far as the neutron damage experiments are concerned, 3 cm and 7 cm borated wax are inserted between the source and the lead plate, respectively. The dewar outside the lead cylinder can hold 25 litres of liquid nitrogen, which is utilized for cooling the Ge crystal during the experiments.
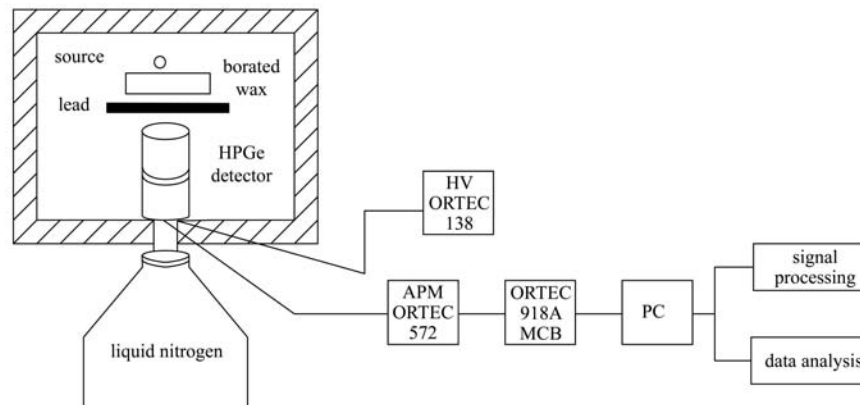

Fig. 1. The schematic of the setup geometry. The HPGe detector is depicted on the left of the plot, which is enclosed by a lead cylinder. The Pu-C source is denoted by a circle; the lead plate and borated wax plate are denoted by the black and the blank rectangles, respectively. The components of the spectrometer system are also indicated schematically at the right of the plot (refer to text for more details).

The p-type[1] HPGe detector is used for the experiments that follow. To obtain the gamma spectrum, a spectrometer system is needed and consists of an ORTEC 138 high voltage power supply, an ORTEC 237 P preamplifier, an ORTEC 572 amplifier and an ORTEC 918 multi-channel buffer (MCB). The high voltage used to bias the detector element is 1500 V. The energy resolution of the spectrometer (full width at half maxium, referred to as FWHM hereafter) is 1.80 keV for 1332 keV peak of ^{60}Co, the relative detection efficiency is 20%.

3 Measurement of the Pu-C source

Figure 2 shows the gamma spectrum of the Pu-C source measured by the HPGe detector. The three peaks indicate the detection of, from right to left, the full-energy, the single-escape and the double-escape modes marked as (a), (b) and (c), respectively. These
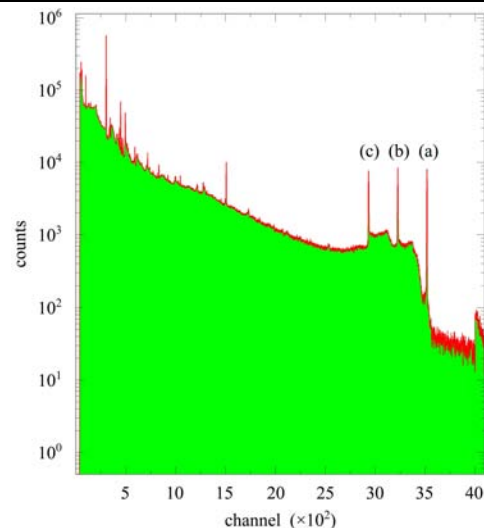

Fig. 2. The gamma spectrum of the Pu-C source. The three peaks indicate the detection of, from right to left, the full-energy, the single-escape, and the double-escape modes as marked (a), (b) and (c) respectively.

---

1) Based on the energy band theory, a certain amount of trivalent impurity integrates itself into the Ge crystal lattice and there will not be enough electrons to fill the valence band. Thus extra holes are left in the crystal. The trivalent impurities perturb the band structure by creating an additional state, which is close to the valence band. Electrons in the valence band are easily excited into this extra level, leaving extra holes. The holes then become the major charge carriers and is called a p-type Ge detector. However when the impurity is pentavalent, an electron is left in the crystal. The electron acts as the major charge carrier and this kind of crystal is called an n-type detector.

peaks can be fitted with the Gaussian function as presented in Fig. 3 (a), (b) and (c), respectively. Based on the ^{60}Co calibration result, the energy for the full-energy peak is determined as 6133.78 keV, the energy resolution is 8.13 keV, which is consistent with the results in Refs. [12, 17] within one σ. The energy positions for the single-escape peak and the double-escape peak fitted using the same function above are 5624.38 keV and 5113.41 keV, the corresponding energy resolutions are 9.38 keV and 9.09 keV, respectively. The three peaks cover the high energy region from 5.1 MeV to 6.1 MeV, which is crucial for high energy calibration as far as τ-charm physics is concerned.

As a calibration source, the Pu-C source should be investigated carefully. The precision of the three peaks position of the Pu-C source may affect the accuracy of the energy measurement system. As pointed out in Ref. [18], the precision of the measured peak position is dependent on the counts of the peak and its width (FWHM),

$$\sigma \sim \text{FWHM}/\sqrt{N}. \qquad (4)$$

The more statistics, the more accurate of the peak position. However, exposure to the Pu-C source for long time will cause a neutron induced reaction and degradation in the germanium detector. In a future experiment, about 10000 events are needed for the calibration work.
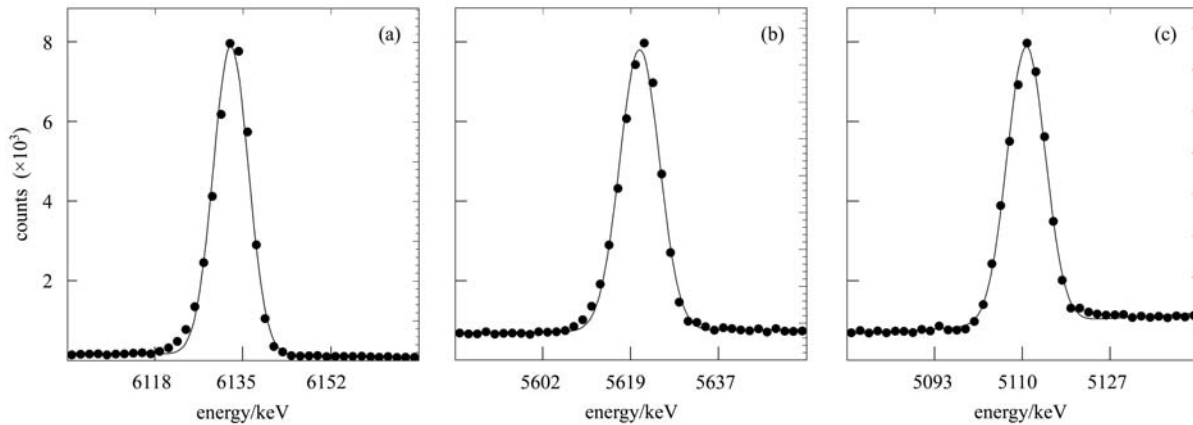

Fig. 3. (a) The full-energy peak; (b) The single-escape peak; (c) The double-escape peak. The three peaks of the Pu-C source can be fitted with the standard Gaussian. Based on the ^{60}Co calibration result, the energy positions for the full energy-peak, the single-escape peak and the double-escape peak are 6133.78 keV, 5624.38 keV and 5113.41 keV, the corresponding energy resolutions are 8.13 keV, 9.38 keV and 9.09 keV, respectively.

4   Neutron irradiation damage

4.1   Experiment results

Table 1 summarizes the experimental results, including radiation time, FWHM, the full width at the one-fifth of the maxium (referred to as FWFM hereafter) and the count rate of the HPGe detector. In order to keep the same precision of the peak position, the counts of every file in the interest region is required to be greater than 40000. Clearly, the FWHM of the detector is almost 8.13 keV when an accumulated fluence of neutron is as low as 2×10^7 n/cm². For the estimation of the dose, the Pu-C source is simplified as a point source. The shape of the full energy peak is a pure Gaussian distribution at both the low and the high energy side as shown in Fig. 4 (a) solid line. However, the values of FWFM further increases, which means that the FWFM can describe the change of shape more precisely than the FWHM value.

As shown in Table 1, a prominent energy resolution degradation occurs after the detector receives radiation fluence of 2×10^7 n/cm². The exponential tail can be seen at the low energy side of the peak and a Gaussian shape is maintained at the high energy side, as seen in Fig. 4 (a) dotted line. As the neutron flux exposures increase successively, the deterioration becomes progressively more serious. The influence of the detector working temperature is eliminated by filling the dewar with liquid nitrogen and keeping the detector sufficiently cooled. The FWHM of the full energy peak is 9.11 keV, which is clearly increased when the detector is subject to a dose of 6.5×10^7 n/cm². When the accumulated neutron fluence reaches 1.66×10^8 n/cm², the FWHM of the full

energy peak is 14.18 keV, nearly twice the original value.

When the detector is subject to an integrated neutron fluence of 1.5×10^8 n/cm^2, a 3 cm borated wax shielding is placed in front of the Pu-C source. The wax is used to slow the fast neutron to a thermal neutron, a 5% boron[1] and 1 mm cadmium (Cd) plate inserted between the lead and the wax is used to absorb the thermal neutron. The small amount of shielding makes no discernable reduction in the neutron damage effects to the detector (see the simulation part). However, the net count rate of 0.50 count per second (cps) decreases to 1/4 of the former one (2.00 cps). Also a thicker borated wax of 7 cm [19] is arranged in our experiment. The net count rate is very small, the typical value is about 0.15 cps. Clearly the distance between the detector and the source is too large and the efficiency is too low to be tolerable.

Table 1. Summary of the experimental results, including the radiation time, integrate neutron dose, FWHM, FWFM and count rate.

Rad. time/h	n/cm^2	FWHM/keV	FWFM/keV	gross/net count rate/cps
1.50	1.53×10^6	8.13	12.83	2.11/1.93
7.35	7.51×10^6	8.11	13.04	2.16/1.96
13.18[1]	1.35×10^7	8.29	13.20	2.10/1.93
19.54	2.00×10^7	8.23	13.51	2.10/1.91
30.45	3.11×10^7	8.61	14.18	2.21/2.00
43.02	4.40×10^7	8.80	15.09	2.26/2.03
50.00	5.11×10^7	9.01	15.47	2.28/2.01
63.99[2]	6.54×10^7	9.11	16.24	2.27/2.01
77.20	7.89×10^7	9.58	17.62	2.27/2.01
83.82	8.57×10^7	9.75	17.83	2.31/2.00
97.08	9.92×10^7	10.26	19.00	2.23/1.98
110.33	1.13×10^8	10.58	20.41	2.23/1.96
123.70	1.26×10^8	10.58	20.84	2.37/2.01
137.26	1.40×10^8	11.94	23.88	2.30/2.01
150.96	1.54×10^8	11.89	23.22	2.31/2.00
160.81	1.61×10^8	13.27	24.20	0.76/0.50
166.81	1.63×10^8	12.90	24.67	0.74/0.49
172.81[3]	1.66×10^8	14.18	27.42	0.75/0.49
183.03	1.67×10^8	17.51	30.92	0.37/0.15

[1] the FWHM for Co-60 1332 keV peak is 4.94 keV.   [2] the FWHM for Co-60 1332 keV peak is 6.22 keV.   [3] the FWHM for Co-60 1332 keV peak is 8.34 keV.
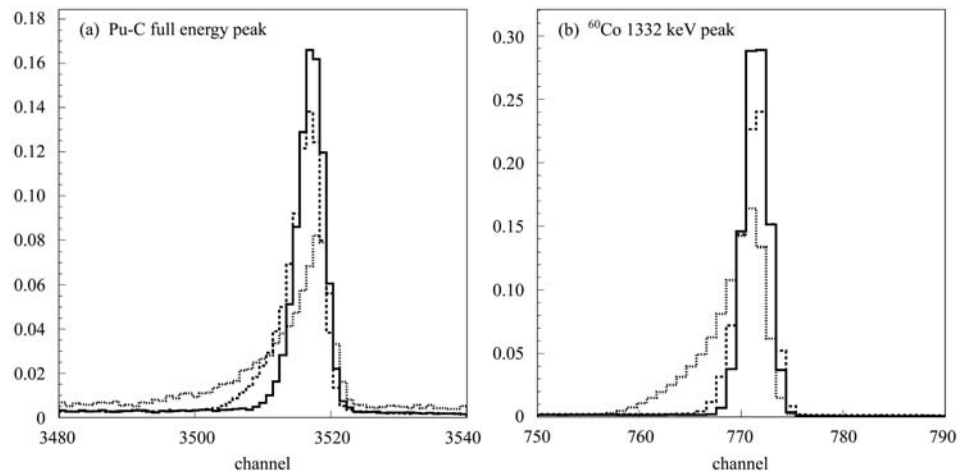

Fig. 4. (a) Pu-C full energy peak; (b) ^{60}Co 1332 keV peak. Variation of the FWHM before and after the neutron radiation. The number of events is normalized. The solid line denotes the FWHM measured by the detector before radiation. The dotted line denotes the FWHM when the HPGe detector is subjected to a dose of 6.5×10^7 n/cm^2. The dashed line presents the FWHM when the accumulated radiation dose is 1.66×10^8 n/cm[1].

---

1) Zhang Qing-Jiang, Private Communication.

When the measurement of the Pu-C source is not carried out, the detector is monitored frequently using a ^{60}Co source at the same position as the Pu-C source. The gamma ray spectra of the ^{60}Co 1332 keV peak are taken to evaluate the performance of the detector as a function of accumulated neutron fluence. The FWHM is listed in Table 1 as a footnote and comparison between the ideal and the damaged distribution is presented in Fig. 4 (b). Before the experiment, the cobalt 1332 keV peak is stable and its FWHM is 4.94 keV[1]. After the detector is subject to a dose of 6.5×10^7 n/cm^2, the FWHM of the peak increased to 6.22 keV. When the accumulated neutron fluence reaches 1.66×10^8 n/cm^2, the FWHM of the ^{60}Co 1332 keV increased to 8.34 keV.

4.2 Damage repairing

Neutron damage to HPGe was noticed and studied two decades ago. Some studies focus on the p-type detector while others on the n-type detector. It is well-known that the p-type detector is more susceptible to fast neutron damage than the n-type one. However, generally speaking, the principle and methods suitable for one type of detector are applicable to the other one too. Therefore, in the following study no special emphasis is placed on the type of detector.

4.2.1 Damage mechanism

The Ge crystal is subject to damage when exposed to fast neutrons with a dose greater than 10^7 n/cm^2. Neutrons knock Ge-atoms out of their lattice sites and lead to the creation of lattice defects like amorphous clusters and isolated defects (Frenkel defects) [20], all of them become trapping centers for carriers, electrons (for n-type detector) or holes (for p-type detector). During a charge collection process, some fraction of the charge carriers, which were created by the absorption of a gamma-quantum, is lost at those trapping sites. The measured pulse height is therefore smaller and this event is recorded in the energy spectrum at lower energies. The line shape of the gamma peaks exhibits the characteristic low-energy tail, which deteriorates the energy resolution.

It is worth stressing that the p-type germanium coaxial detector should not be used in any situation subject to significant radiation damage. This point was anticipated because the defects produced by neutron irradiation of germanium act predominantly as hole traps [21, 22].

4.2.2 Software correction

One method was developed to correct gamma-spectroscopy data for effects of charge carrier trapping in neutron-damaged coaxial HPGe-detector [23]. In addition to the pulse height, the risetime of each signal is measured with standard nuclear spectroscopy electronics and both data are recorded on tape.

According to the analysis of Ref. [23], the pulse height of the output signal from the detector is, in principle, proportional to the absorbed gamma-energy E_γ. If the creation of the electron-hole pairs by the absorption of a gamma-quantum takes place at a certain radius r_0 inside the active region, the pulse height of a neutron-damaged HPGe detector will strongly depends on r_0. The reason is that some charge carriers are lost at the neutron induced trapping sites and the amount of the charge lost thus depends on the drift length of the charge carriers. Moreover, it is noticed that the risetime τ_{rise} increases with increasing radius r_0. This relation between the radius r_0 and the risetime τ_{rise} offers the possibility of determining r_0 from a measurement of τ_{rise}.

With this basic idea the correction method is as follows:

1) Measure the pulse height E and the risetime τ_{rise} of each event.

2) Make a suitable calibration and find a correction function $\beta(\tau_{\text{rise}})$ so that:

$$E_\gamma = (1 + \beta(\tau_{\text{rise})}) \cdot E \ . \tag{5}$$

3) Correct each event with Eq. (5).

After the correction, the resolution of gamma-spectroscopy data from a neutron-damage coaxial HPGe-detector can be enhanced considerably. As pointed out in Ref. [23], the FWHM at 1333 keV was improved from 2.71 keV to 2.24 keV. The low energy tails of the gamma-peaks could be corrected, so that a nearly symmetric line shape was obtained.

4.2.3 Anneal repairing

The annealing technique is primarily used to eliminate the residual defects in the growth of Ge Crystals [24]. Even for dislocation-free (DF) Ge[2], residual defects such as lattice vacancy complexes may exist. There are many kinds of vacancy complexes,

---

1) This value is different from that given in the document. Two reasons cause this difference: the first is the interested energy region, up to 7–8 MeV, which is much wider than the usual measurement, therefore, the values of amplifier and shaping time are different from those recommended to obtain the best resolution. The second is that the detector has served for 13 years, so the long time usage makes its properties much worse.

2) During the growth of materials, if the thermal distributions in crystal is not homogeneous enough, the number of dislocations will be increased thereby relaxing thermal stress.

for example, monovacancy (V_1), divacancy (V_2) and divacancy hydrogen (V_2H). For DF crystal, the V_2 is much higher because there are no dislocations to serve as sinks for the annihilation of V_1s. Also, there are fewer or no larger clusters present, since these presumably form at the dislocation jogs or forks in crystals with dislocation. Thus, the principal defect present is the V_2, which is equivalent to the carrier trapping centers. These frozen lattice defects in the crystal are expected to respond to an annealing treatment. However, such a heat treatment must be carried out with precautions and subtle details should be taken into account. The most important factors are the temperature and the cooling process.

The defects due to neutron damage are similar to those of vacancy complexes, both of which degrade the resolution of Ge detector. Therefore, an annealing technique is also adopted for the resolution recovery of a Ge detector suffering from neutron irradiation damage. Here, it should be noted that the annealing temperature for irradiation damage is usually much lower than that for crystal growth [24, 25].

4.2.4 HPGe repairing

Ref. [20] pointed out that after annealing at the normal or higher temperature, the HPGe detector's properties can be recovered. The HPGe detector is taken out from the dewar and remains at the normal temperature (18 ℃) for 4 days, allowing the atoms diffuse freely. The detector shows significant resolution degradation after annealing, as reported in Ref. [26, 27]. Then, we sent the detector to a germanium detector expert for repair. After annealing at about 100 ℃ to 120 ℃ for three days, the resolution is fully recovered.

5 Shielding simulation

In order to obtain a count rate that is as high as possible, we minimize the distance between the source and the detector. However, if the distance is too small, severe radiation damage may be inflicted on the detector. A Monte Carlo simulation is helpful for designing the protection due to the difficulty of experiment.

The simulation calculations on the interaction of neutrons with germanium are carried out using the GEANT 4.9.0 framework. The precision of many low energy process models in this package has improved, so it has been applied in many nuclear experiments. As far as neutron shielding in this paper is concerned, the correlative dominant processes are low energy nuclear processes. The binary cascade model[1] is added in order to simulate the inelastic interaction of hadrons. Furthermore, the default models of low energy inelastic processes for certain particles, and the default models of low energy electromagnetic processes and elastic processes are used so that the interactions between neutrons and atoms in nucleus such as capture and fission are also included.

Implications from the calculation and space environment conditions lead to special requirements for the neutron and detector setup. During the simulation, the set of protection conditions is simplified as a spherical shell type: the center is the Pu-C source, the outermost is the HPGe detector, the shielding layers lie between the source and the detector.

According to the design, three materials (cadmium, lead and 5% borated wax) are considered for protective shielding. Firstly, we consider the borated wax only, the variation of the penetrated rate of neutron with the thickness of wax is shown in Fig. 5. Then, a 1 mm cadmium plate and a 2 mm lead plate are inserted between the wax and the detector. Clearly, the cadmium or lead is almost useless for neutron shielding. According to Fig. 5, even though the thickness of the borated wax is 15 cm, about 27% of the neutrons penetrate through the shielding layer, with which the acceptance of the gamma detection is only about 1.2%.
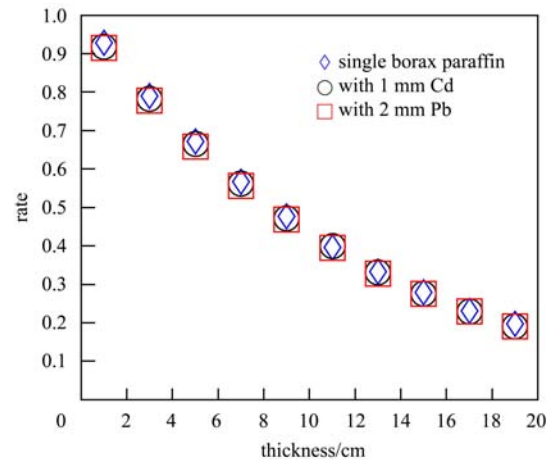

Fig. 5. The relation between the penetrated rate of neutron and the thickness of borated wax.

When the thickness of the Cd is increased, the protective effect is enhanced. A 10 cm Cd plate with 1 cm borated wax will decrease the penetration rate to 32%, while the rate will be 16% when the thickness of borated wax is increased to 9 cm. In fact, the

1) Geant4 manual. http://geant4.web.cern.ch/geant4/support/index.shtml.

shielding effect of 19 cm borated wax is better than that of 10 cm Cd plate plus 9 cm borated wax.

6   Conclusion and discussion

Three results are reported in this paper: firstly, using a Pu-C source as the calibration source for a HPGe detector is studied and measured spectroscopy clearly displays the three peaks, full energy peak, single-escape peak and double-escape peak. All of them can be fitted with fairly high accuracy, which indicates the excellent calibration feature of Pu-C source.

Secondly, the neutron damage effect due to a Pu-C source on a HPGe detector is studied in detail. The relation between the radiation dose and detector resolution is obtained. The annealing methods for Ge crystal are reviewed and the annealing results for the utilized detector are also given.

Thirdly, the neutron shielding for Ge detector protection is studied with help of a Monte Carlo simulation based on the Geant4 package. The relation

between the thickness of borated wax and radiation dose are obtained, which is very promising for further detector protection.

However, as far as beam energy measurement system is concerned, the significance of the present work lies in the warning which we received from the neutron damage effect on HPGe detector. Such damage was beyond our preliminary expectation. Compared with the Pu-C source, the irradiation at NCP within the storage ring tunnel is more complicated and more dangerous. The present results makes it important for us to know as much as possible the radiation dose at NCP, especially the neutron radiation background distribution around the area where the HPGe detector will be located.

References

1 CHAO Kuang-Ta, WANG YI-FANG. Internation Journal of Modern Physics A (Suppl. Issue 1), 2009, **24**: 1

2 YUAN Chang-Zheng, ZHANG Bing-Yun, QIN Qing. HEP & NP, 2002, **26**: 1201 (in Chinese)

3 FU Cheng-Dong, MO Xiao-Hu. Chinese Phyusics C, 2008, **32**: 776

4 MO Xiao-Hu. Nucl. Phys. B (Proc. Suppl.), 2007, **169**: 132

5 WANG You-Kai, MO Xiao-Hu, YUAN Chang-Zheng et al. Nucl. Instrum. Methods A, 2007, **583**: 479

6 Achasov M N, Blinov V E, Bogomyagkov A V et al. Nuclear Physics B (Proc. Suppl.), 2009, **189**: 366

7 Preliminary Design Report of Accelerator BEPCII, Second version, 2003 (in Chinese) Refer to http://acc-center.ihep.ac.cn/bepcii/bepcii.htm

8 MO Xiao-Hu, FU Cheng-Dong et al. Chinese Physics C, 2008, **32**: 995

9 Rullhusen P, Artru X, Dhez P. Novel Radiation Source Using Relativistic Electrons, Singpore: World Science Publishing, 1998

10 Landau L D, Lifshitz E M. Relativistic Quantum Mechanics. Oxford: Pergamon, 1971

11 MO Xiao-Hu, ZHANG Jian-Yong, ZHANG Tian-Bao et al. Chinese Physics C (HEP & NP), 2009, **33**: 914

12 Dickens J K, Baybarz R D. Nucl. Instrum. Methods, 1970, **85**: 143

13 Mason J P. Nucl. Instrum. Methods A, 1985, **241**: 207

14 DING Xi-Xiang, DING Sheng-Yao, WANG You-Mei et al. Atom Energy Science and Technology, 1996, **30**: 361 (in Chinese)

15 WANG Song-Lin, HUANG H X, RUAN Xi-Chao et al. Chinese Physics C (HEP & NP), 2009, **33**: 378–382

16 Haller E E. IEEE Transactions on Nuclear Science, 1982, **NS-29**: 1109

17 Klein P, Kuske P, Thornagel R et al. Nucl. Instrum. Methods A, 2002, **486**: 545

18 CHANG T B, WANG S Y, WANG H D. Nucl. Instrum. Methods A, 1993, **325**: 196–204

19 MA Chong-Zhi et al. Manual of Radioisotope. Beijing: Science Press, 1979. 462 (in Chinese)

20 Raudorf T W, Trammell R C, Wagner S et al. IEEE Trans. on Nucl. Sci., 1984, **NS-31**(1): 253

21 Borrel V, Kandel B, Albernhe F et al. Nucl. Instrum. Methods A, 1999, **430**: 348

22 Koenig Z M, Gunnink R et al. UCRL-JC–105888

23 Eschenauer M. Nucl. Instrum. Methods A, 1994, **340**: 364

24 Haller R N. IEEE Transactions on Nuclear Science, 1984, **NS-31**: 320

25 Kandel et al. Nucl. Instrum. Methods A, 1999, **430**: 363

26 Fourches N et al. IEEE Transactions on Nuclear Science, 1991, **NS-38**: 1728

27 Darken J S. Nucl. Instrum. Methods B, 1993, **74**: 523